JMEPEG (2006) 15:182-186
DOI: 10.1361/105994906X95841

1059-9495/$19.00

# Chemically Functionalized Carbon Nanotubes and Their Characterization Using Thermogravimetric Analysis, Fourier Transform Infrared, and Raman Spectroscopy

*E. Titus, N. Ali, G. Cabral, J. Gracio, P. Ramesh Babu, and M.J. Jackson*

*(Submitted November 4, 2005; in revised form December 23, 2005)*

**This article reports key findings on the chemical functionalization of carbon nanotubes (CNT). The functionalization of chemical vapor-deposited CNT was carried out by treating tubes with polyvinyl alcohol through ultrasonication in water with the aid of a surfactant. The surfactant is expected to promote the unbundling of aggregated CNT. The characterization of functionalized samples using thermogravimetric analysis, Fourier transform infrared spectroscopy, and Raman spectroscopy revealed that the CNT were functionalized by the interaction of carboxylic acid and hydroxyl groups. From the characterization studies, it is apparent that there is a strong interaction between these functional groups and the covalently bonded carbon in the CNT network. The functionalization process enabled good CNT dispersion in the solution, and the CNT remained in suspension for many days. To support the effective functionalization of the tubes, the interaction of functionalized CNT with Ni ions is also demonstrated.**

**Keywords** carbon nanotubes, chemical vapor deposition, dispersion, functionalization

## 1. Introduction

Chemical functionalization of carbon nanotubes (CNT) is an area that has received considerable world-wide research interest (Ref 1, 2). In particular, from a chemical point of view, pure CNT are of relatively less practical importance due to the absence of any active functional groups, despite the fact that CNT have a seemingly useful structural motif (Ref 3-6). The functionalization of CNT has been pursued in a number of cases (Ref 7-9), either through direct chemical modification or through chemical bonding. However, many of the chemical-bonding procedures resulted in long-chain CNT compounds, which act as a barrier to the anchoring of foreign elements onto the surface of the CNT in a specific orientation. Despite the few disadvantages (Ref 10-12), chemical modifications at the CNT surface is regarded as the best method to functionalize the tubes because it is known that chemical reactions can take place at defect sites on a CNT in a colloidal state. Therefore, the uniform dispersion of CNT has a potential role in the functionalization of CNT. When CNT are mixed and agitated with suitable solvents, they disperse to create a stable suspension. The homogeneous dispersion of CNT in polyvinyl alcohol (PVA) and CNT–PVA composites has been studied by a number of researchers (Ref 13-15). In this article, the effective functionalization of CNT using PVA (Nanolab, Newton, MA) in the presence of a novel surfactant is discussed. The results of Fourier transform infrared (FTIR) spectroscopy, Raman spectroscopy (RS), and thermogravimetric analysis (TGA) are presented to establish the functionalization of the CNT in the polymer/surfactant system by interaction with the covalent carbon of the CNT. The analysis showed several interesting features that have not been reported earlier. The FTIR spectroscopy and TGA results were correlated with the authors new results, which were obtained from the nickel sulfate/CNT/polymer/surfactant system.

## 2. Experimental

The CNT were deposited onto 0.6 mm thick Cu substrates, which were electroplated with Ni. The substrates were polycrystalline in nature and had a commercial purity of ~98%. They were polished with SiC abrasive paper to improve their roughness. The electroplating of Ni coatings onto the substrate was performed in an electroplating bath. The substrates were used as a cathode, and a Ni electrode served as the anode. Commercial grade nickel sulfate was used as the electrolyte in the direct current (dc) electroplating process. The bath temperature was maintained at 40 °C, and the pH was constant at 4. The Ni layers, 50 nm in thickness, were treated in $NH_3$ plasma for 5 min prior to CNT growth. The $NH_3$ plasma treatment was necessary for the formation of nano-sized nickel catalyst particles, which potentially act as seeds for subsequent CNT growth using chemical vapor deposition. Methane ($CH_4$) and hydrogen ($H_2$) were used as precursor gases for the CNT growth, where the flow rates were kept constant at 6 and 40 standard cubic centilitres/min (sccm), respectively. The PVA (98% hydrolyzed) used in this investigation was obtained from Aldrich (St. Louis, MO). Different ratios of CNT and PVA

This paper was presented at the fourth International Surface Engineering Congress and Exposition held August 1-3, 2005 in St. Paul, MN.

**E. Titus, N. Ali, G. Cabral,** and **J. Gracio,** Department of Mechanical Engineering, University of Aveiro, 3810-193 Aveiro, Portugal; **P. Ramesh Babu,** Polymer Research Center, Department of Physics, Trinity College, Dublin 2, Ireland; and **M.J. Jackson,** Birck Nanotechnology Center and College of Technology, Purdue University, West Lafayette, IN 47907-2021. Contact e-mail: jacksomj@purdue.edu.

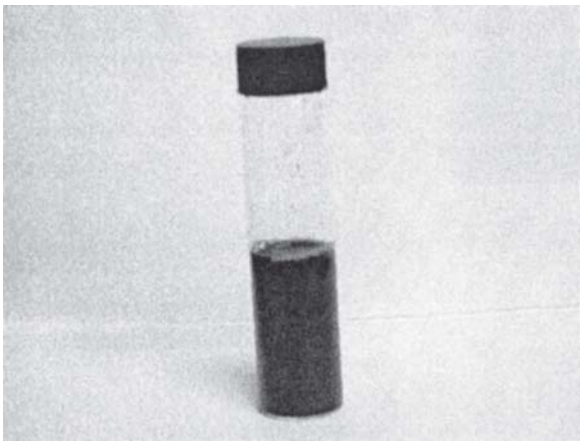

**Fig. 1** Dispersibility behavior of a CNT in an aqueous solution of PVA and nanodisperse after being stored for 4 weeks

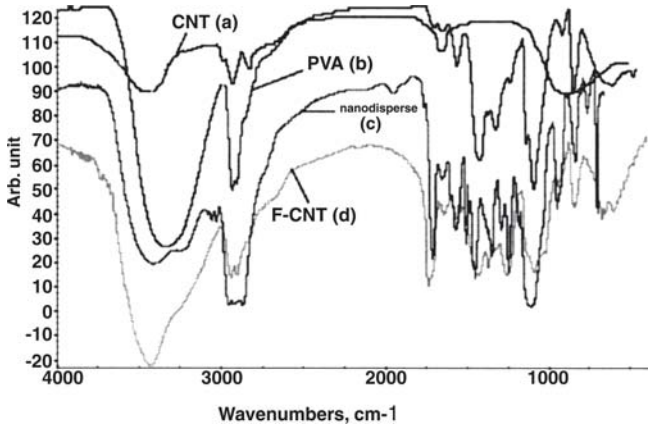


**Fig. 2** (a) The FTIR spectra of as-grown CNT, (b) PVA, (c) nanodisperse, and (d) F-CNT

(e.g., 1 to 100 mg) were dissolved in 0.1 mL of novel nanodisperse, which is a mixture of surfactants of 20 to 50% poly-(oxy-1,2-ethandiyl, α-[nonylphenyl]-ω hydroxy, 2 to 10% tetramethyl-5-decyne-2,47,9), and 50 mL of deionized water. The resultant mixture was ultrasonicated for 10 min (sonic tip 120 W and 60 kHz with 20% amplitude). The suspension was in the form of a colloidal solution that remained in that state for 1 month without settling (Fig. 1). The functionalized CNT (F-CNT)/nickel sulfate suspension was synthesized by the ultrasonic agitation of CNT, PVA, and nanodisperse in a nickel sulfate-aqueous bath for 5 h.

The suspended solution was kept for four weeks and later was filtered to separate the metal-F-CNT (MF-CNT) composites. For the FTIR spectroscopy analysis, the separated CNT were washed with distilled water several times to remove the unadsorbed PVA and surfactant. TGA was performed using a PerkinElmer Pyris I TGA thermobalance (Wellesley, MA). With the TGA experiments, the sample was heated in air from 30 to 900 °C at a heating rate of 10 °C/min. The FTIR spectroscopy analysis was performed using a Nicolet NEXUS (Thermo-Electron Corp., Waltham, MA) bench machine with 128 scans. The Raman spectra were recorded at room temperature using a Renishaw 1000 (New Mills, Gloucestershire, U.K.) micro-Raman system equipped with a Leica microscope (Carl Zeiss, Thornwood, U.K.). The 50× magnifying objective of the microscope focused a laser beam onto a spot of ~1 μm diameter. The excitation wavelength used was 514.5 nm from an $Ar^+$ ion laser. A grating of 1800 lines/mm was used in all measurements, which allowed a resolution of ~1 line/cm.

## 3. Experimental Results and Discussion

To identify the functional groups of CNT, FTIR studies have been performed in the range 400 to 4000/$cm^{-1}$. FTIR spectroscopy has been used extensively in the structural determination of molecules. Its application in the study of surface chemistry has provided one of the most direct means of observing the interactions and perturbations that occur at the surface during adsorption and in determining the structure of the adsorbed species. Some FTIR spectra are shown in Fig. 2 for CNT (curve a), PVA (curve b), nano-disperse (curve c), and an F-CNT treated with PVA and nanodisperse (curve d). The characteristic vibrational modes of CNT, C = C (1650/cm) and O-H (3400/cm), are apparent in the spectrum shown in Fig. 2 (curve a). The C = C vibrations occur due to the internal defects, and the O-H vibration is associated with the amorphous carbon because amorphous carbon easily forms a bond with atmospheric air. However, the intensity of this O-H peak is relatively lower and shows that a lesser amount of amorphous carbon formed during growth. A typical PVA spectrum (Fig. 2, curve b) consists of major peaks centered at 3328, 2938, 1569, and 1423/cm, which are related to the O-H (stretching), C-H, O-H (bending), and C-C bonding (Ref 16). The spectrum for the nanodisperse consists of major peaks that are centered at around 3400, 1716, 1455, and 1250/cm, which are due to the OH and COOH bonds. However, the F-CNT exhibits a higher intensity O-H peak that is centered at 3441/cm with a major shift from CNT, polymer, and nanodisperse O-H peaks.

Surfactants (i.e., surface-active molecules) are a class of molecules exhibiting a strong tendency to adsorb at interfaces. They are characterized by the presence of both polar (hydrophilic) and nonpolar (hydrophobic) moieties. They typically have a hydrophobic chain, known as a *tail*, and a hydrophilic group, known as a *head*. At the interfaces, the molecule can be oriented in different ways. In general, the hydrophilic head is directed toward the bulk water, and the hydrophobic chains will orient themselves to avoid the water. The PVA also acts as a surfactant in the presence of water. The hydrophilic part in water overcomes the van der Waals attraction, and, therefore, there is no self-aggregation of PVA molecules in water. Surfactants, however, tend to form micellar structures, which is a common phenomenon that was originally observed in the self-association process of the surface-active materials in aqueous solutions (Ref 17). Although micellization represents a self-association phenomenon, in general it is conventionally limited to the self-association initiated by the hydrophobic-hydrophilic imbalance. It is likely that the presence of a polymer would result in the formation of small aggregates (micelles) of surfactant by adsorbing onto the long chain of the PVA. The adsorption of surfactant on a polymer alkyl chain was reported by Dibakar and Shah (Ref 18). Because CNT are hydrophobic, there is a strong possibility for the hydrophobic interaction between the CNT and the hydrophobic head of the surfactant, consequently resulting in the adherence of the surfactant to the CNT. The possible interactive mechanism of the polymer, the surfactant, and the CNT is schematically shown in Fig. 3. On

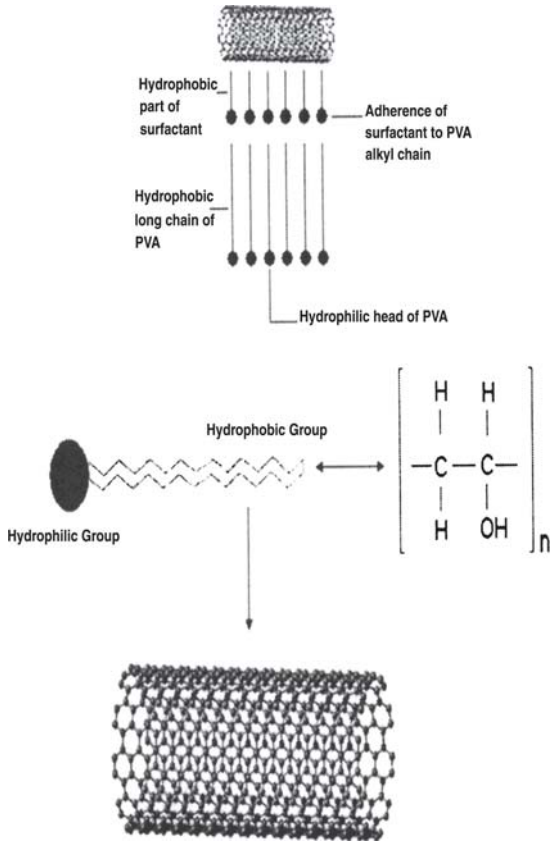


**Fig. 3** Schematic diagram showing the interaction of the surfactant with CNT

the addition of the surfactant to the polymer solution, some of the surfactant micelles are bound to, or adsorbed onto, the polymer chain.

The hydrophilic groups of the PVA chain form an ion-dipole association with the ionic head groups of the surfactant, and a net local electrostatic charge is developed. An electrostatic force exists between the surfactant and the covalent carbon. The interaction is evidenced by the shift of the O-H bond of the surfactant to a higher wave number. The shift is also observed in the O-H bending region. The C-H bonds (~2900/cm) of PVA and the nanodisperse appeared in the same position in the F-CNT spectrum with almost similar intensity. This shows that the C-H bond does not play any role in the interaction between CNT and PVA-nanodisperse. The strong C-H bonds of PVA-nanodisperse were unable to form a bond with the covalent carbon of the CNT, and therefore, there was no vibrational energy transaction between them. It was interesting to observe the appearance of new peaks centered at around 1737 and 1258/cm in the F-CNT sample, which were due to the COOH group (Ref 19). This is assumed to be formed as a result of the interaction between the surfactant and the CNT. The interaction is confirmed by the shift in peak position compared with the original surfactant spectrum. It was assumed that the steric hindrance of the OH and COOH functionalized groups is responsible for the suspension of the CNT in the polymer solution.

To support these findings, FTIR spectroscopy analysis was performed on an MF-CNT, which was prepared as described in the Experimental Results and Discussion section. Metal composites are expected to be useful in a diverse range of appli-

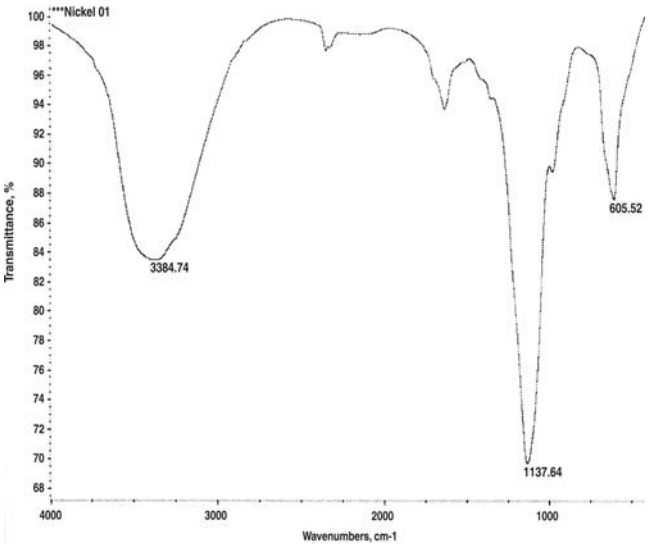


**Fig. 4** The FTIR spectrum of MF-CNT

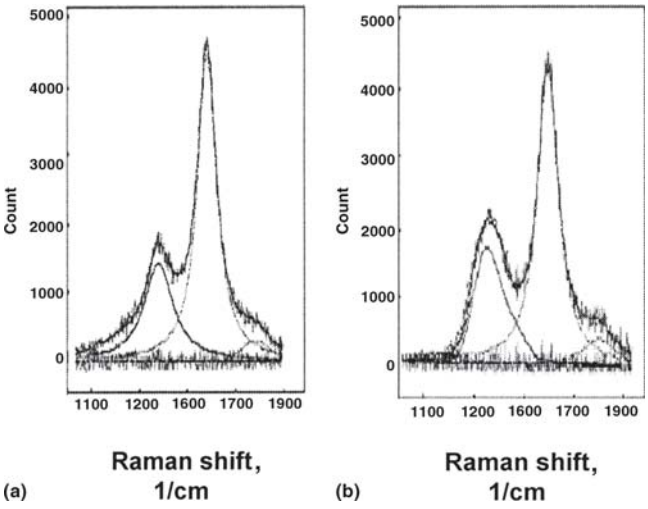


**Fig. 5** Raman spectra of (a) CNT and (b) F-CNT

cations, such as molecular electronics, photocatalysis, and solar energy conversion, and as probes for scanning force microscopy. However, very few investigations have been carried out on CNT/metal composites (Ref 20-22). The main difficulty in the formation of this composite is the anchoring of the metal onto its surface through a specific bond or interaction. Although few researchers have tried the electrodeposition of metals (Ref 23) onto CNT, the adherence of the metal is the cause of the problem for researchers. The uncontrolled electrodeposition can even affect its properties inversely, due to the high-melting point of the metal and the possible reverse solubilization of CNT. From the FTIR spectroscopy analysis (Fig. 4) of the metal-interacted sample, two strong peaks were found to be related to the C = C vibrations at 1132 and 1680/cm. However, the peak positions were shifted and were found to be different from both the as-grown CNT and the F-CNT, which is a clear indication of the interaction of the F-CNT with the metal. The Ni being a positive ion can potentially interact with the charged F-CNT system.

Raman scattering is a powerful technique to characterize

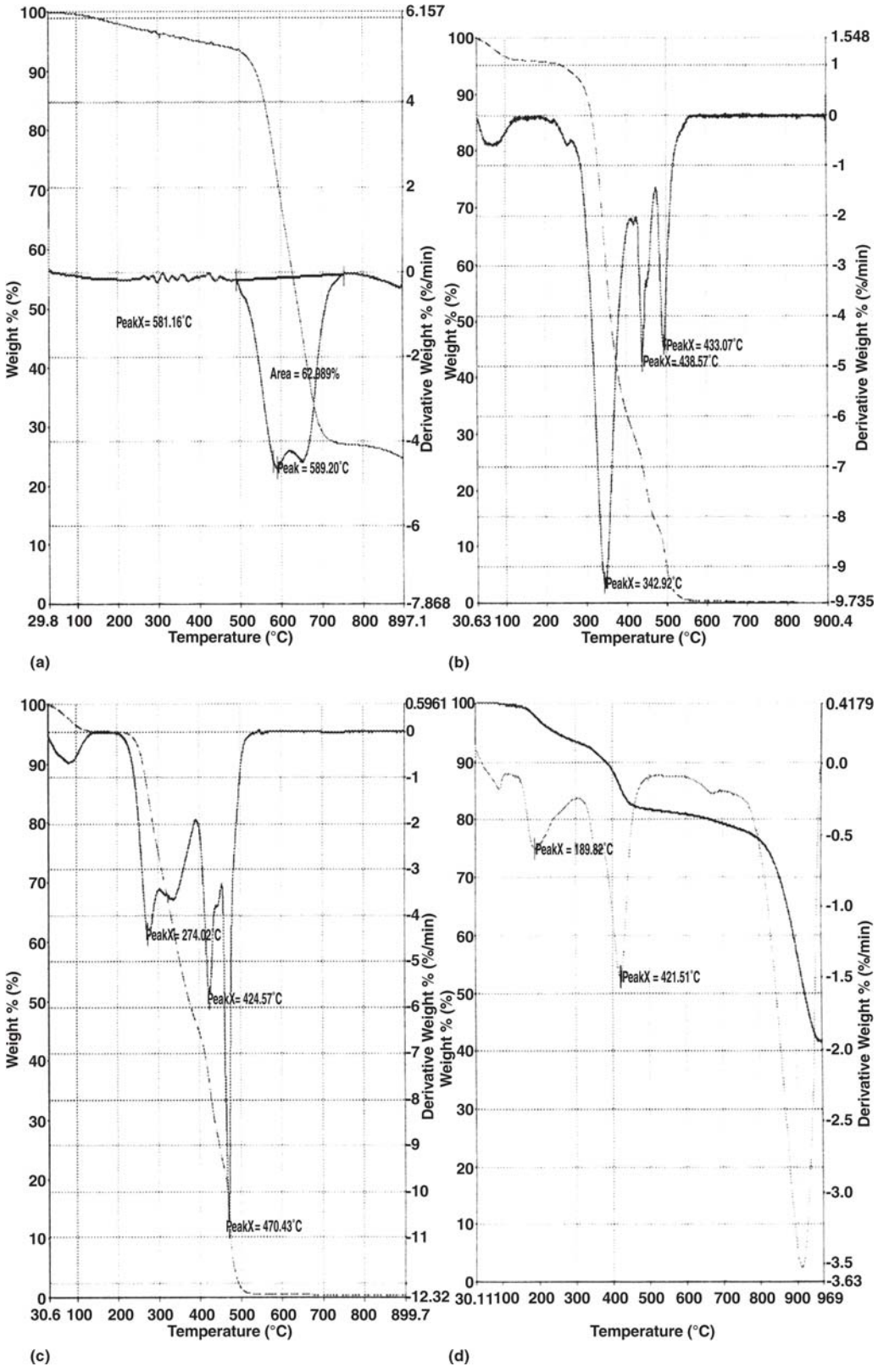


**Fig. 6** Thermogravimetric thermogram (dashed lines) and differential thermogram (solid lines) of (a) CNT, (b) PVA, (c) F-CNT, and (d) MF-CNT

and probe the structure-property relationship in both CNT and polymers. Figure 5 shows the typical Raman spectra of CNT (Fig. 5a) and F-CNT (Fig. 5b). Two strong scattering peaks were observed for both CNT and F-CNT centered at 1345 and 1590/cm, respectively. The band centered at 1590/cm has been assigned to the graphite-like tangential mode "G" band, and the so-called "D" band centered at 1345/cm has been attributed to disorder or to $sp^3$-hybridized carbon in the hexagonal framework of the nanotube walls. The intensity ratio of the band at ~1590/cm to that at 1345/cm (G to D) reflects the proportion

and purity of the CNT in the samples. Although the shape and positions of peaks in the spectra are fairly similar to each other, the value of the G-to-D ratio displayed some regular and substantial changes, which can reveal something about the structural information of the sample. The increase in the relative intensity of the disordered mode can be attributed to the increased number of structural defects and to the $sp^3$ hybridization of carbon for chemically induced disruption of the hexagonal carbon order in the nanotubes after treatment with the polymer. This may be due to the attachment of carboxylic acid groups to the CNT (Ref 15).

To obtain further information, TGA was performed. Figure 6 shows a comparison of the mass losses of as-grown CNT (Fig. 6a), PVA (Fig. 6b), and F-CNT (Fig. 6c). The solid and the dashed dotted lines correspond to thermogravimetric and differential thermogravimetric (DTG) curves, respectively. A ~5% mass loss observed at around 250 °C in pure PVA is attributed to the moisture loss. The onset of degradation of pure PVA occurs at 342.92 °C, and the thermogram is characterized by a mass loss of 65%. The mass loss at 439.57 and 493.07 °C may be due to the decomposition of structurally transformed PVA at higher temperatures. The onset temperature of F-CNT (470 °C) was higher compared with raw PVA, although it was lower compared with as-grown CNT. The thermogram displayed a mass loss of 55%. A mass loss of multiwalled CNT-COOH at 460 °C has been reported by Zhao et al. (Ref 24). Although the TGA of MF-CNT (Fig. 5) displays a different behavior, it shows a sharp DTG curve at 421.51 °C, which is believed to be due to the functionalization of CNT. The shift in the curve may be due to the difference in the degree of interaction. The curves at 80 and 189.82 °C, respectively, are assigned based on the mass loss of water and Ni. It is noteworthy to mention that both the F-CNT and MF-CNT show extremely different thermal behavior compared with the as-grown CNT, which has a typical mass loss of amorphous carbon and CNT at 580 and 650 °C, respectively.

## 4. Conclusions

The present work demonstrates the effective functionalization of CNT using PVA in the presence of a surface-active agent. The research findings show that the OH and COOH functional groups are assumed to be attached to the covalent carbon of CNT. Well-dispersed CNT were obtained, and the dispersion is due to the steric hindrance of the OH and COOH groups that were functionalized to CNT. The special attainment of this work is in the simplified method for the functionalization of CNT in the aqueous phase at normal temperature without any complex reactions. The presence of functional groups attached to CNT was confirmed by TGA and FTIR spectroscopy. The modification of CNT and their extended properties may be promising for use in applications such as polymer-CNT composites and coatings.

## References


1. D. Quian, E.C. Dickey, R. Andrews, and T. Rantell, Laod Transfer and Deformation Mechanisms in Carbon Nanopolystyrene Composites, *Appl. Phys. Lett.,* 2000, **76,** p 2868-2873
2. D. Bhaskaran, J.W. Mays, and M.S. Bratcher, Polymer Grafted MWCNT Through Surface Polymerization, *Angew. Chem., Int. Ed. Engl.,* 2004, **43,** p 2138-2142
3. J. Chen, M.A. Hamon, H. Hu, Y. Chen, A.M. Rao, P.C. Eklund, and R.C. Haddon, Solution Properties of Multiwalled Carbon Nanotubes, *Science,* 1998, **282,** p 95-98
4. H. Kong, C. Gao, and D. Yan, Controlled Functionalization of MWCNT by In Situ Atom Transfer Radical Polymerization, *J. Am. Chem. Soc.,* 2004, **126,** p 412-413
5. J.L. Hudson, M.J. Casavent, and J.M. Tour, Water Soluble, Exfoliated, Non-Roping SWCNTs, *J. Am. Chem. Soc.,* 2004, **126,** p 11158-11159
6. A. Star, J.F. Stoddart, M. Diehl, A. Boukai, E.W. Wong, and X. Yang, Preparation and Properties of Polymer Wrapped SWCNTs, *Angew. Chem., Int. Ed. Engl.,* 2001, **40,** p 1721-1725
7. S. Kumar, T.D. Dang, F.E. Arnold, A.R. Bhattacharya, B.G. Min, and X. Zhang, Synthesis, Structures, and Synthesis of PBO/SWCNT Composites, *Macromolecules,* 2002, **35,** p 9039-9043
8. W. Haung, S. Fernando, Y. Lin, B. Zhou, L.F. Allard, and Y.P. Sun, Preferential Stabilization of Smaller SWCNT in Sequential Functionalized Reactions, *Langmuir,* 2003, **19,** p 7084-7088
9. M. Holzinger, J. Abraham, P. Whelan, R. Graupner, L. Ley, F. Henrich, M. Kappes, and A. Hirsch, Functionalization of SWCNTs with (R-) Oxycarbonyl Nitrenes, *J. Am. Chem. Soc.,* 2003, **125,** p 8566-8580
10. H. Pan, L. Liu, Z.X. Guo, L. Dai, F. Zhang, D. Zhu, R. Czerw, and D.L. Carroll, Carbon Nanotubols From Mechanochemical Reactions, *Nano Lett.,* 2003, **3,** p 29-32
11. H.J. Choi, S.J. Park, S.T. Kim, and M.S. Jhon, Functional Carbon Nanotubes Using CVD Methods, *Diamond Relat. Mater.,* in press
12. H. Kong, P. Luo, C. Gao, and D. Yan, Polymer Electrolyte Functionalization of MWCNTs, *Polymer,* 2005, **46,** p 2472-2485
13. G. Jiang, L. Wang, C. Chen, X. Dong, T. Chen, and H. Yu, Study on Attachment of Branched Molecules on Multiwalled Carbon Nanotubes, *Mater. Lett.,* 2005, **59,** p 2085-2089
14. A.G. Rozhin, Y. Sakakibara, M. Tokumoto, H. Kataura, and Y. Achiba, Near Infra-Red Optical Properties of SWCNTs Embedded in Polymer Film, *Thin Solid Films,* 2004, **464,** p 368-372
15. M.C. Paiva, B. Zhou, K.A.S. Fernando, Y. Lin, J.M. Kennedy, and Y.P. Sun, Mechanical and Morphological Characterization of Polymer Nanocarbon Composites From CNTs, *Carbon,* 2004, **42,** p 2849-2854
16. D. Hwan Jung, Y.K. Ko, and H.T. Jung, Nanocarbon Composites Made From CNTs, *Mater. Sci. Eng.,* 2004, **24,** p 117-125
17. E.D. Goddard, Surface Functionalization of Colloid Surfaces, *Colloids Surf.,* 1986, **19,** p 255-260
18. D. Dibakar and D.O. Shah, Effect of Polyethylene Glycols on Micellar Stability of Sodium Dodecyl Sulfate, *Langmuir,* 2001, **17,** p 7233-7236
19. M. Liu, Y. Yang, T. Zhu, and Z. Liu, Surface Characterization of Carbon Nanotubes, *Carbon,* in press
20. Q. Han and A. Zettl, Coating SWCNTs With Tin Oxide, *Nano Lett.,* 2003, **3,** p 681-683
21. J.H. Shi, Y.J. Qin, W. Wu, X.L. Li, Z.X. Guo, and D.B. Zhu, In Situ Synthesis of CdS Nanoparticles on SWCNTs, *Carbon,* 2004, **42,** p 455-458
22. S. Banerjee and S.S. Wong, Synthesis and Characterization of CNT Heterostructures, *Nano Lett.,* 2002, **2,** p 195-200
23. C.M. Schneider, B. Zhao, R. Kozhuharova, S. Groudeva-Zotova, T. Mühl, M. Ritschel, I. Mönch, H. Vinzelberg, D. Elefant, and A. Graff, Towards Molecular Spintronics, *Diamond Relat. Mater.,* 2004, **13,** p 215-220
24. C. Zhao, L. Ji, Huiju, G. Hu, G. Hu, S. Zhang, M. Yang, and Z. Yang, Functionalized CNTs Containing Isocyanate Groups, *J. Solid State Chem.,* 2004, **177,** p 4394-4398